

Topological Color-Hall Insulators: SU(3) Fermions in Optical Lattices

Man Hon Yau and C. A. R. Sá de Melo

School of Physics, Georgia Institute of Technology, Atlanta, 30332, USA

(Dated: April 30, 2019)

We discuss the emergence of topological color insulators in optical lattices as quantum phases of SU(3) ultra-cold neutral fermions. We construct the Chern matrix and classify all insulating phases in terms of three topological invariants: the charge-charge, the color-charge and the color-color Chern numbers. Our classification transcends that of SU(2) systems which require only the charge-charge (charge-Hall) and spin-charge (spin-Hall) Chern numbers. To illustrate the topological classification of the insulating phases of SU(3) fermions, we construct phase diagrams of chemical potential and color-orbit parameter versus color-flip fields for fixed magnetic flux ratio.

The identification of topological invariants for charged SU(2) fermions has been very important in the distinction between trivial and non-trivial insulators found in condensed matter physics. The integer quantum Hall effect is a typical example of the importance of topological invariants, where the quantum Hall conductance (charge-charge response) is proportional to an integer [1] in two-dimensional lattices at high magnetic fields. This topological invariant, known as the TKKN [1] integer, is also identified as the first Chern number of a U(1) principal fiber bundle on a torus [2]. The TKKN integer counts the number and chirality of edge states in two-dimensional SU(2) systems with open boundary conditions, as indicated by the bulk-edge correspondence [3, 4].

More recently, topological insulators, with zero quantum Hall and non-zero quantum spin-Hall conductances, were found to exist in graphenelike two-dimensional lattices without Zeeman or magnetic fields, but in the presence of spin-orbit coupling [5]. When spin is conserved, the quantization of the spin-charge (spin-Hall) response is the result of spin-dependent TKNN integers having opposite values, that is, $C_{\text{TKNN}}^{\uparrow} = -C_{\text{TKNN}}^{\downarrow}$, in which case spin-orbit coupling plays a pivotal role. This state of matter is coined the quantum spin-Hall phase, and exhibits spin-filtered edge states carrying opposite currents for opposite spins, while possessing a bulk energy gap. Extensions of these findings for finite Zeeman [6] and magnetic [7] fields in SU(2) graphenelike lattices have indicated that quantum spin-Hall phases can survive the breaking of time-reversal symmetry.

However, in spite of a deeper understanding of topological properties of SU(2) fermions in two-dimensional lattices found in condensed matter systems, very little is known about the topological properties of neutral SU($N \geq 3$) fermions, such as ^{173}Yb , that have been loaded into optical lattices [8–13]. Many experiments involving cold atoms have focused on studying topological properties of neutral SU(2) systems due to their direct connections to their charged SU(2) cousins. A few experiments have attempted to explore neutral SU(2) systems in fictitious magnetic and spin-orbit fields with the goal of studying the analogues of the quantum charge-charge (charge-Hall) and spin-charge (spin-Hall) effects [14, 15].

In this paper, we show that neutral SU(3) fermions are qualitatively different from their neutral or charged SU(2) relatives. By labeling the internal states of the atoms as colors, we find that the topological insulating phases are characterized by a set of three topological invariants: charge-charge, color-charge, and color-color Chern numbers. This is in contrast with SU(2) systems, where only charge-charge (charge-Hall) and spin-charge (spin-Hall) Chern numbers are necessary to classify topological insulators [6]. We show examples of our classification for phase diagrams of neutral SU(3) fermions loaded into two-dimensional lattices and in the presence of fictitious magnetic, color-flip and color-orbit fields.

Hamiltonian: To describe topological phases of SU(3) fermions loaded into two-dimensional optical lattices, we start from the Hamiltonian

$$\hat{H} = - \sum_{\mathbf{r}, \boldsymbol{\eta}_{\ell}} t_{\ell} \psi^{\dagger}(\mathbf{r}) e^{-i\boldsymbol{\theta}_{\ell}} \psi(\mathbf{r} + \boldsymbol{\eta}_{\ell}) - h_x \sum_{\mathbf{r}} \psi^{\dagger}(\mathbf{r}) \mathbf{J}_x \psi(\mathbf{r}), \quad (1)$$

where t_{ℓ} are hopping energies along the $\ell = \{x, y\}$ direction, and h_x plays the role of a color-flip field along the x direction. The phase operators $\boldsymbol{\theta}_{\ell}$ describe the effect of artificial color-orbit coupling $\boldsymbol{\theta}_x = k_T \eta_x \mathbf{J}_z$, with momentum transfer k_T and artificial gauge field $\boldsymbol{\theta}_y = \mathcal{A}_y \eta_y \mathbf{1}$, where $\mathcal{A}_y = eH_z x / \hbar c$ plays the role of the y component of an artificial vector potential with dimension of inverse length. Here, H_z is identified as a synthetic magnetic field along the z -axis. The vector potential \mathcal{A}_y may be generated by laser assisted tunneling [14, 15], while the color-dependent momentum transfer k_T and color-flip field h_x may be created via counter-propagating Raman beams [16] or via radio-frequency chips [17]. The vectors $\boldsymbol{\eta}_{\ell} = \eta_{\ell} \hat{\boldsymbol{\ell}}$, with $\eta_x = \pm a_x$ and $\eta_y = \pm a_y$, indicate the position $\mathbf{r} + \boldsymbol{\eta}_{\ell}$ of nearest neighbors with respect $\mathbf{r} = (x, y)$, where fermion creation operators are defined by three-component vectors $\psi^{\dagger}(\mathbf{r}) = [\psi_R^{\dagger}(\mathbf{r}), \psi_G^{\dagger}(\mathbf{r}), \psi_B^{\dagger}(\mathbf{r})]$ with color $c = \{R, G, B\}$ (Red, Green and Blue). The unit cell lengths are a_x (a_y) along the x (y) direction, $\hat{\boldsymbol{\ell}} = \{\hat{\mathbf{x}}, \hat{\mathbf{y}}\}$ are the corresponding unit vectors, while the operators \mathbf{J}_x and \mathbf{J}_z are pseudospin-1 matrices with states $\{\uparrow, 0, \downarrow\}$ representing colors $\{R, G, B\}$, respectively, and $\mathbf{1}$ is the identity matrix.

Under the color-gauge transformation $\psi(\mathbf{r}) = e^{ik_T x \mathbf{J}_z} \tilde{\psi}(\mathbf{r})$, the Hamiltonian of Eq. (1) becomes

$$\hat{H} = - \sum_{\mathbf{r}, \eta_\ell} t_\ell \tilde{\psi}^\dagger(\mathbf{r}) e^{-i\tilde{\theta}_\ell} \tilde{\psi}(\mathbf{r}) - h_x \sum_{\mathbf{r}} \tilde{\psi}^\dagger(\mathbf{r}) \tilde{\mathbf{J}} \tilde{\psi}(\mathbf{r}), \quad (2)$$

with $\tilde{\theta}_x = 0$, $\tilde{\theta}_y = \theta_y$, and $\tilde{\mathbf{J}} = \mathbf{J}_x \cos(k_T x) + \mathbf{J}_y \sin(k_T x)$. When $h_x = 0$ the color-orbit coupling can be gauged away (color-gauge symmetry), since the resulting Hamiltonian and its eigenvalues are independent of k_T .

We transform the second quantization Hamiltonian of Eq. (1) into the first quantization Hamiltonian matrix

$$\hat{\mathbf{H}} = \begin{pmatrix} \varepsilon_R(\hat{\mathbf{k}}) & -h_x \sqrt{2} & 0 \\ -h_x \sqrt{2} & \varepsilon_G(\hat{\mathbf{k}}) & -h_x / \sqrt{2} \\ 0 & -h_x / \sqrt{2} & \varepsilon_B(\hat{\mathbf{k}}) \end{pmatrix} \quad (3)$$

that describes a color generalization of the original Harper's Hamiltonian for SU(2) fermions [18]. The matrix elements are

$$\varepsilon_R(\hat{\mathbf{k}}) = -2t_x \cos[(\hat{k}_x - k_T)a_x] - 2t_y \cos[(\hat{k}_y - \mathcal{A}_y)a_y] \quad (4)$$

corresponding to the kinetic energy of the R state,

$$\varepsilon_G(\hat{\mathbf{k}}) = -2t_x \cos[(\hat{k}_x a_x)] - 2t_y \cos[(\hat{k}_y - \mathcal{A}_y)a_y] \quad (5)$$

corresponding to the kinetic energy of the G state, and

$$\varepsilon_B(\hat{\mathbf{k}}) = -2t_x \cos[(\hat{k}_x + k_T)a_x] - 2t_y \cos[(\hat{k}_y - \mathcal{A}_y)a_y] \quad (6)$$

corresponding to the kinetic energy of the B state. Lastly, h_x is a color-flip field along the x direction, whose physical origin is a Rabi term that couples Red and Green, as well as, Green and Blue internal states of the atom. The Hamiltonian matrix in Eq. (3) acts on a three-color wavefunction $\Psi(\mathbf{r}) = [\Psi_R(\mathbf{r}), \Psi_G(\mathbf{r}), \Psi_B(\mathbf{r})]^T$, where T indicates transposition.

Rewriting Eq. (3) in terms of spin-1 matrices \mathbf{J}_ℓ , with $\ell = \{x, y, z\}$, leads to

$$\hat{\mathbf{H}} = \varepsilon_G(\hat{\mathbf{k}})\mathbf{1} - h_x \mathbf{J}_x - h_z(\hat{\mathbf{k}})\mathbf{J}_z + b_z(\hat{\mathbf{k}})\mathbf{J}_z^2 \quad (7)$$

where h_x plays the role of a Zeeman field along the x axis in spin-space, $h_z(\hat{\mathbf{k}}) = [\varepsilon_B(\hat{\mathbf{k}}) - \varepsilon_R(\hat{\mathbf{k}})]/2$ represents momentum dependent Zeeman field along the z axis in spin-space, and $b_z(\hat{\mathbf{k}}) = [\varepsilon_B(\hat{\mathbf{k}}) + \varepsilon_R(\hat{\mathbf{k}})]/2 - \varepsilon_G(\hat{\mathbf{k}})$ describes a momentum dependent quadratic Zeeman field along the z axis in spin-space. The explicit forms of the operators are $h_x(\hat{\mathbf{k}}) = 2t_x \sin(k_T a_x) \sin(\hat{k}_x a_x)$ and $b_z(\hat{\mathbf{k}}) = 4t_x \sin^2(k_T a_x / 2) \cos(\hat{k}_x a_x)$. The term $b_z(\hat{\mathbf{k}})\mathbf{J}_z^2$ describes a momentum dependent color-quadrupole (or pseudo-spin-quadrupole) coupling, reflecting the entanglement of momentum and tensorial degrees of freedom [19–21]. The presence of the color fields h_x , $h_z(\hat{\mathbf{k}})$ and $b_z(\hat{\mathbf{k}})$ breaks SU(3) symmetry [22], however the color-gauge transformation restores SU(3) symmetry when

$h_x = 0$ for any value of k_T . The term $b_z(\hat{\mathbf{k}})\mathbf{J}_z^2$ is absent for SU(2) fermions in the presence of spin-orbit coupling, but, here, it plays a very important role in the determination and classification of topological insulating phases that emerge between degenerate SU(3) symmetric color insulators at $h_x = 0$ and fully polarized color insulators at $h_x \rightarrow \infty$.

Eigenspectrum: We choose first a cylindrical geometry with periodic boundary conditions along the y direction, and a finite number M_x of sites along the x direction. In this case, k_y is a good quantum number, while k_x is not, leading to the color-dependent Harper's matrix

$$\mathbf{H} = \begin{pmatrix} \mathbf{A}_{m-2} & \mathbf{B} & \mathbf{0} & \mathbf{0} & \mathbf{0} \\ \mathbf{B}^* & \mathbf{A}_{m-1} & \mathbf{B} & \mathbf{0} & \mathbf{0} \\ \mathbf{0} & \mathbf{B}^* & \mathbf{A}_m & \mathbf{B} & \mathbf{0} \\ \mathbf{0} & \mathbf{0} & \mathbf{B}^* & \mathbf{A}_{m+1} & \mathbf{B} \\ \mathbf{0} & \mathbf{0} & \mathbf{0} & \mathbf{B}^* & \mathbf{A}_{m+2} \end{pmatrix}, \quad (8)$$

which has a tridiagonal block structure coupling neighboring sites $(m-1, m, m+1)$ along the x direction, with $x = ma_x$, and discrete translational symmetry along the y axis. The matrices \mathbf{A} , \mathbf{B} and the null matrix $\mathbf{0}$ consist of 3×3 blocks with entries labeled by internal color states $\{R, G, B\}$ or pseudo-spin-1 states $\{\uparrow, 0, \downarrow\}$. The size of the space labeled by the site index m is M_x , thus the total dimension of the matrix \mathbf{H} in Eq. (8) is $3M_x \times 3M_x$. The matrix indexed by position $x = ma_x$ is

$$\mathbf{A}_m = \begin{pmatrix} \mathbf{A}_{mR} & -h_x / \sqrt{2} & 0 \\ -h_x / \sqrt{2} & \mathbf{A}_{mG} & -h_x / \sqrt{2} \\ 0 & -h_x / \sqrt{2} & \mathbf{A}_{mB} \end{pmatrix},$$

with $\mathbf{A}_{mR} = \mathbf{A}_{mG} = \mathbf{A}_{mB} = -2t_y \cos(k_y a_y - 2\pi m \alpha)$. Here, $\alpha = \Phi / \Phi_0$ is the ratio of the magnetic flux through a lattice plaquette $\Phi = H_z a_x a_y$ to the flux quantum $\Phi_0 = hc/e$. The matrix containing the color-orbit coupling is

$$\mathbf{B} = \begin{pmatrix} -t_x e^{-ik_T a_x} & 0 & 0 \\ 0 & -t_x & 0 \\ 0 & 0 & -t_x e^{ik_T a_x} \end{pmatrix},$$

where k_T ($-k_T$) corresponds to the momentum transfer along the x direction for state R (B), while the momentum transfer for state G is zero.

We consider $M_x = 50$ sites along the x direction, with three states $\{R, G, B\}$ per site, but periodic boundary conditions along the y direction. The eigenvalues $E_{n_\beta}(k_y)$ are labeled by a discrete band index n_β and by momentum k_y , and are functions of the color-orbit coupling k_T , color-flip field h_x and flux ratio $\alpha = \Phi / \Phi_0$. In Fig. 1, we show $E_{n_\beta}(k_y)$ for flux ratio $\alpha = 1/3$ in four cases. In Fig. 1(a) with $k_T a_x = 0$ and $h_x / t_y = 0$, there are three sets of degenerate bulk bands connected by color-degenerate edge states. In Fig. 1(b) with $k_T a_x = \pi/8$ and $h_x / t_y = 0$, the plots are identical to case (a) because of the color-gauge symmetry allows gauging away the color-orbit coupling. Notice in (a) and (b) that the bulk band gaps are connected by edge states at filling

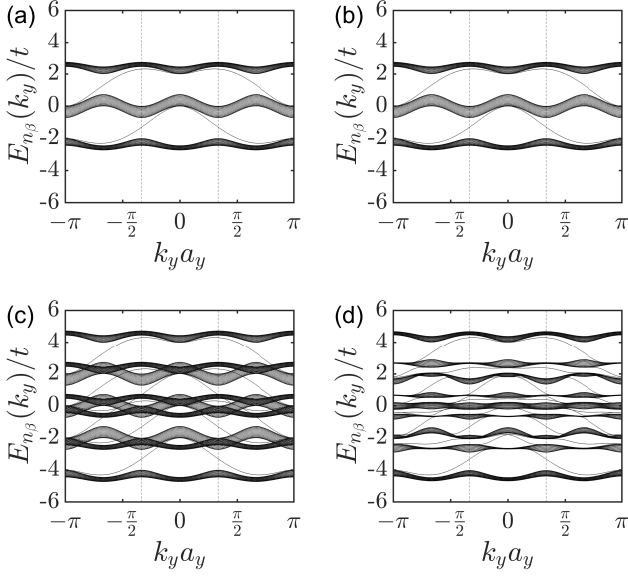


FIG. 1: Eigenvalues $E_{n\beta}(k_y)$ of the color-dependent Harper's matrix versus $k_y a_y$ for magnetic flux ratio $\alpha = 1/3$ and $t_x = t_y$. The parameters are: (a) $k_T a_x = 0$ and $h_x/t_y = 0$, (b) $k_T a_x = \pi/8$ and $h_x/t_y = 0$, (c) $k_T a_x = 0$ and $h_x/t_y = 2$, (d) $k_T a_x = \pi/8$ and $h_x/t_y = 2$. The vertical dashed lines located at $k_y a_y = \pm\pi/3$ indicate the boundaries of the magnetic Brillouin zone. The bulk bands have periodicity $2\pi/3a_y$, and the edge bands have periodicity $2\pi/a_y$ along the k_y direction.

factors $\nu = \{1, 2\}$. In Fig. 1 with (c) $k_T a_x = 0$ and $h_x/t_y = 2$, there are nine sets of bulk bands with regions of overlap because color-degeneracies are only partially lifted by the color-flip field, and the bulk bands are also connected by color-dependent edge states. Bulk gaps are now present at $\nu = \{1/3, 1, 2, 8/3\}$. In Fig. 1(d) with $k_T a_x = \pi/8$ and $h_x/t_y = 2$, there are nine sets of bulk bands connected by color-dependent edge states, but residual bulk band overlaps are lifted by color-orbit coupling, that is, because $k_T a_x \neq 0$. Therefore, new insulating states arise at filling factors $\nu = \{2/3, 4/3, 5/3, 7/3\}$ due to the presence of $h_z(\hat{\mathbf{k}})$ and $b_z(\hat{\mathbf{k}})$ in Eq. (7).

Each eigenvalue $E_{n\beta}(k_y)$ has associated eigenstates $|k_y, n\beta, \beta\rangle$, where β is a mixed-color index, reflecting the mixing of color components induced by h_x and k_T . The eigenstates can be written as a linear combination $|k_y, n\beta, \beta\rangle = \sum_{n c_x} u_{n\beta n}^{\beta c_x} |k_y, n, c_x\rangle$, where c_x represents the color basis with quantization axis along h_x , and n is the band index in the absence of color-orbit coupling. The β index has three assigned values $\{\uparrow, \emptyset, \downarrow\}$ or $\{C, M, Y\}$ (Cyan, Magenta, Yellow) to indicate the mixed-color nature of the state.

Chern matrix: To characterize the topological nature of the insulating phases, we impose the generalized boundary condition on the many-particle wavefunction $\Psi(\mathbf{r}_{1c}, \dots, \mathbf{r}_{jc} + \mathbf{L}_\ell, \dots, \mathbf{r}_{N_p c}) = e^{i\phi_\ell c} \Psi(\mathbf{r}_{1c}, \dots, \mathbf{r}_{jc}, \dots, \mathbf{r}_{N_p c})$, where \mathbf{r}_{jc} is the position of the i^{th} particle of color c , N_p is the total number of particles, $\mathbf{L}_\ell = M_\ell a_\ell \hat{\ell}$

is the length vector along $\ell = \{x, y\}$ direction, and ϕ_ℓ^c is the phase twist [23] along ℓ for color c . Under the transformation $\tilde{\Psi}(\mathbf{r}_{1c}, \dots, \mathbf{r}_{jc}, \dots, \mathbf{r}_{N_p c}) = e^{-i \sum_{j,c} [\phi_{xc} \frac{x_{jc}}{M_x a_x} + \phi_{yc} \frac{y_{jc}}{M_y a_y}]} \Psi(\mathbf{r}_{1c}, \dots, \mathbf{r}_{jc}, \dots, \mathbf{r}_{N_p c})$ with $0 \leq \phi_{\ell c} < 2\pi$, the wavefunction $\tilde{\Psi}(\mathbf{r}_{1c}, \dots, \mathbf{r}_{jc}, \dots, \mathbf{r}_{N_p c})$ is periodic in $\phi_{\ell c}$, and we can define the Chern matrix [24]

$$C_{cc'} = \frac{i}{4\pi} \iint d\phi_{xc} d\phi_{yc'} \mathcal{F}_{xy}(\phi_{xc}, \phi_{yc'}), \quad (9)$$

where the purely imaginary *curvature* function

$$\mathcal{F}_{xy}(\phi_{xc}, \phi_{yc'}) = \left\langle \frac{\partial \tilde{\Psi}}{\partial \phi_{xc}} \left| \frac{\partial \tilde{\Psi}}{\partial \phi_{yc'}} \right. \right\rangle - \left\langle \frac{\partial \tilde{\Psi}}{\partial \phi_{yc'}} \left| \frac{\partial \tilde{\Psi}}{\partial \phi_{xc}} \right. \right\rangle \quad (10)$$

is integrated over the torus $\mathcal{T}_{cc'}$, that is, over the ranges of phase twists $0 \leq \phi_{xc} < 2\pi$ and $0 \leq \phi_{yc'} < 2\pi$. The dimension of the Chern number matrix is 3×3 , since there are three color states $c = \{R, G, B\}$ or three pseudo-spin 1 states $c = \{\uparrow, 0, \downarrow\}$. In passing, we note that the $SU(N)$ generalization for $N > 3$ leads to an $N \times N$ Chern matrix.

The expression given in Eq. (9) is an integer just like in $SU(2)$ systems [25]. Three topological invariants can be obtained from the Chern matrix above. The first invariant is the charge-charge (charge-Hall) Chern number $C_{\text{ch}}^{\text{ch}} = \sum_{cc'} C_{cc'}$. The second is the color-charge (color-Hall) Chern number $C_{\text{ch}}^{\text{co}} = \sum_{cc'} m_c C_{cc'}$, or charge-color Chern number $C_{\text{co}}^{\text{co}} = \sum_{cc'} C_{cc'} m_{c'}$, since $C_{\text{ch}}^{\text{ch}} = C_{\text{co}}^{\text{co}}$. The third topological invariant is the color-color Chern number $C_{\text{co}}^{\text{co}} = \sum_{cc'} m_c C_{cc'} m_{c'}$, where m_c is the color quantum number with $m_R = +1$, $m_G = 0$, and $m_B = -1$, as identified from the pseudo-spin 1 representation $m_\uparrow = +1$, $m_0 = 0$, and $m_\downarrow = -1$.

A simple way to connect these results to conventional $SU(2)$ condensed matter physics of electrons and holes is to look at the current density J_x^λ , where λ refers to either charge or color, that is, $\lambda = \{\text{ch}, \text{co}\}$ and the conductivity tensor $\tilde{\sigma}_{xy}^{\lambda\tau}$ through the generalized relation $J_x^\lambda = \tilde{\sigma}_{xy}^{\lambda\tau} E_y^\tau$, where E_y^τ plays the role of a generalized *electric* field with $\tau = \{\text{ch}, \text{co}\}$. To simplify our notation we drop the xy labels, define the conductivity tensor $\tilde{\sigma}_{xy}^{\lambda\tau} \equiv \tilde{\sigma}_\tau^\lambda$, and work finally with the conductance tensor $\sigma_{xy}^{\lambda\tau} \equiv \sigma_\tau^\lambda$. If we were dealing with fermions with charge e and conserved pseudo-spin 1 projection along a global quantization axis, then the charge-charge (charge-Hall) conductance would be $\sigma_{\text{ch}}^{\text{ch}} = (e^2/h) C_{\text{ch}}^{\text{ch}}$, the color-charge (color-Hall) conductance would be $\sigma_{\text{co}}^{\text{ch}} = (e^2/h)(\hbar/e) C_{\text{co}}^{\text{ch}} = (e/2\pi) C_{\text{co}}^{\text{ch}}$ and the color-color conductance would be $\sigma_{\text{co}}^{\text{co}} = (e/2\pi)(\hbar/e) C_{\text{co}}^{\text{co}} = (\hbar/2\pi) C_{\text{co}}^{\text{co}}$. However, our fermions are really neutral and their colors represent three internal states of the atoms, thus one can only hope to probe the charge-charge (charge-Hall) and color-charge (color-Hall) and color-color Chern numbers in analogy with measurement proposals [26–28] or actual measurements [29, 30] of Chern numbers for atomic systems with one and two internal states.

In the $SU(2)$ case, the topological invariant equivalent to $C_{\text{co}}^{\text{co}}$ is the spin-spin Chern number $C_{\text{sp}}^{\text{sp}} = \sum_\sigma m_\sigma^2 C_{\sigma\sigma}$

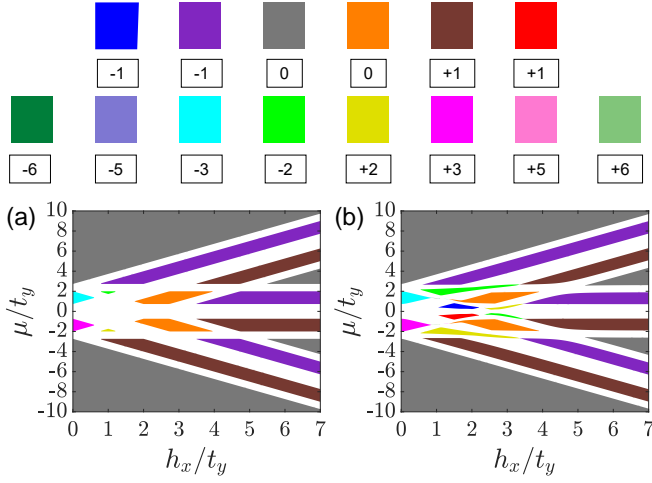


FIG. 2: Phase diagrams of chemical potential μ/t_y versus Zeeman field h_x/t_y for $t_x = t_y$ and color-orbit coupling parameters: (a) $k_T a_x = 0$, (b) $k_T a_x = \pi/8$. The white (non-white) regions correspond to conducting (insulating) phases. The values of the charge-charge (charge-Hall) Chern numbers $C_{\text{ch}}^{\text{ch}}$ for each insulating region are indicated in the legend.

which has the same value as charge-charge (charge-Hall) Chern number $C_{\text{ch}}^{\text{ch}} = \sum_{\sigma} C_{\sigma\sigma}$, since $m_{\sigma}^2 = 1$. Since $C_{\text{sp}}^{\text{sp}}$ does not add any additional information about the topological nature of insulating phases for SU(2) systems, it is sufficient to stop the topological classification at the spin-charge (spin-Hall) level, such as the \mathbb{Z}_2 classification used in the case of quantum spin-Hall phases of graphene-like structures [5, 6]. However, in the SU(3) case, $C_{\text{co}}^{\text{co}}$ provides new topological information and can be used to refine the topological classification of the non-trivial insulating phases. We note that for SU(N) fermions with $N > 3$ flavors, the generalized flavor-flavor Chern number $C_{\text{ff}}^{\text{ff}}$ will also provide additional topological information about the insulating states.

Phase Diagrams: In Fig. 2, we show the phase diagram of chemical potential μ/t_y versus Zeeman field h_x/t_y for fixed value of the magnetic flux ratio $\alpha = 1/3$, hoppings $t_x = t_y$ and two values of the color-orbit parameter: (a) $k_T a_x = 0$, and (b) $k_T a_x = \pi/8$. The white regions indicate conducting phases, while the regions with other colors correspond to insulating phases. The color palette in Fig. 2 indicates the charge-charge (charge-Hall) Chern numbers $C_{\text{ch}}^{\text{ch}}$ associated with the corresponding colored regions. However, $C_{\text{ch}}^{\text{ch}}$ is not sufficient to classify the topological insulating phases of SU(3) fermions for arbitrary $k_T a_x$ and h_x/t_y , as we also need the color-charge (color-Hall) $C_{\text{co}}^{\text{ch}}$ and color-color $C_{\text{co}}^{\text{co}}$ Chern numbers.

In Figs. 2(a) and 2(b), we see our classification at work. The gray regions, occurring at filling factors $\nu = 0, 1, 2, 3$, are topologically trivial with either non-chiral or no edge states at all. They have charge-charge (charge-Hall) Chern number $C_{\text{ch}}^{\text{ch}} = 0$ and also zero color-charge (color-Hall) and color-color Chern numbers $C_{\text{co}}^{\text{ch}} = C_{\text{co}}^{\text{co}} = 0$. The magenta region at $\nu = 1$ has Chern numbers

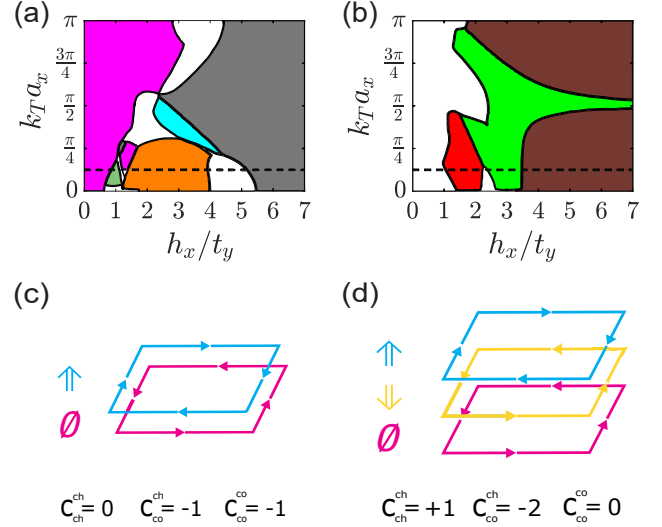


FIG. 3: (Color Online) Phase diagram of color-orbit coupling $k_T a_x$ versus color-flip field h_x/t_y for filling factors $\nu = 1$ in (a) and $\nu = 4/3$ in (b). Dashed lines are shown for $k_T a_x = \pi/8$. The color coding is the same used in Fig. 2. In (c), edge states are shown for the orange region in (a). In (d), edge states are shown for the red region in (b). Corresponding Chern numbers are listed.

$C_{\text{ch}}^{\text{ch}} = +3$, $C_{\text{co}}^{\text{ch}} = 0$ and $C_{\text{co}}^{\text{co}} = +2$, while the cyan region at $\nu = 2$ has Chern numbers $C_{\text{ch}}^{\text{ch}} = -3$, $C_{\text{co}}^{\text{ch}} = 0$ and $C_{\text{co}}^{\text{co}} = -2$. These regions, occurring at low values of h_x/t_y , are the analogue of the traditional quantum Hall phases of SU(2) fermions. However, the yellow region at $\nu = 2/3$ with $C_{\text{ch}}^{\text{ch}} = +2$, $C_{\text{co}}^{\text{ch}} = +1$ and $C_{\text{co}}^{\text{co}} = +1$, and green region at $\nu = 7/3$ with $C_{\text{ch}}^{\text{ch}} = -2$, $C_{\text{co}}^{\text{ch}} = +1$ and $C_{\text{co}}^{\text{co}} = -1$, have no counterparts for SU(2) fermions.

The orange regions, occurring at filling factors $\nu = 1, 2$, have $C_{\text{ch}}^{\text{ch}} = 0$, but, unlike the gray regions, they are topologically non-trivial. Each orange region has two chiral edge states and non-zero $C_{\text{co}}^{\text{co}} = -1$, but they are distinguished further by their color-color Chern number $C_{\text{co}}^{\text{co}}$. The orange region with $\mu < 0$ and $\nu = 1$ has $C_{\text{co}}^{\text{co}} = -1$, however, the orange region with $\mu > 0$ and $\nu = 2$ has $C_{\text{co}}^{\text{co}} = +1$. These are quantum color-Hall states, that is, the SU(3) analogues of the time-reversal broken quantum spin-Hall states that occur in SU(2) fermions.

The phases at high values of h_x/t_y , represented by the brown and purple regions, describe color-polarized insulating states. The brown region at $\nu = 1/3$ has $C_{\text{ch}}^{\text{ch}} = +1$, $C_{\text{co}}^{\text{ch}} = +1$ and $C_{\text{co}}^{\text{co}} = +1$; the brown region at $\nu = 4/3$ has $C_{\text{ch}}^{\text{ch}} = +1$, $C_{\text{co}}^{\text{ch}} = 0$ and $C_{\text{co}}^{\text{co}} = 0$; and the brown region at $\nu = 7/3$ has $C_{\text{ch}}^{\text{ch}} = +1$, $C_{\text{co}}^{\text{ch}} = -1$ and $C_{\text{co}}^{\text{co}} = +1$. The purple region at $\nu = 2/3$ has $C_{\text{ch}}^{\text{ch}} = -1$, $C_{\text{co}}^{\text{ch}} = -1$ and $C_{\text{co}}^{\text{co}} = -1$; the purple region at $\nu = 5/3$ has $C_{\text{ch}}^{\text{ch}} = -1$, $C_{\text{co}}^{\text{ch}} = 0$ and $C_{\text{co}}^{\text{co}} = 0$; and the purple region at $\nu = 1/3$ has $C_{\text{ch}}^{\text{ch}} = -1$, $C_{\text{co}}^{\text{ch}} = +1$ and $C_{\text{co}}^{\text{co}} = -1$. In Fig. 2(b), there are additional insulating phases induced by color-orbit coupling, such as the red region at

$\nu = 4/3$ with $C_{\text{ch}}^{\text{ch}} = +1$, $C_{\text{co}}^{\text{ch}} = -2$ and $C_{\text{co}}^{\text{co}} = 0$; the blue region at $\nu = 5/3$ has $C_{\text{ch}}^{\text{ch}} = -1$, $C_{\text{co}}^{\text{ch}} = -2$ and $C_{\text{co}}^{\text{co}} = 0$; the green region at $\nu = 4/3$ has $C_{\text{ch}}^{\text{ch}} = -2$, $C_{\text{co}}^{\text{ch}} = 0$ and $C_{\text{co}}^{\text{co}} = 0$; and the yellow region at $\nu = 5/3$ has $C_{\text{ch}}^{\text{ch}} = +2$, $C_{\text{co}}^{\text{ch}} = 0$ and $C_{\text{co}}^{\text{co}} = 0$.

We plot phase diagrams of color-orbit coupling parameter $k_x a_x$ versus color-flip field h_x/t_y for $\nu = 1$ in Fig. 3(a) and for $\nu = 4/3$ in Fig. 3(b). Two phases not yet discussed arise in Fig. 3(a), a light green region with $C_{\text{ch}}^{\text{ch}} = +6$, $C_{\text{co}}^{\text{ch}} = -1$ and $C_{\text{co}}^{\text{co}} = +3$, and a cyan region with $C_{\text{ch}}^{\text{ch}} = -3$, $C_{\text{co}}^{\text{ch}} = -1$ and $C_{\text{co}}^{\text{co}} = -1$, while no new phases arise in Fig. 3(b). In order to relate SU(3) fermions to their SU(2) cousins, we show schematically edge states in Fig. 3(c) linked to the orange region in Fig. 3(a), and edge states in Fig. 3(d) linked to the red region Fig. 3(b).

Conclusions: For SU(3) fermions in optical lattices,

we showed that the classification of topological color insulators requires three topological invariants: the charge-charge, the color-charge and the color-color Chern numbers. We analyzed SU(3) fermions in the presence of artificial magnetic, color-flip and color-orbit fields, and indicated that our classification transcends that of SU(2) fermions, where only charge-charge (charge-Hall) and spin-charge (spin-Hall) Chern numbers are necessary to characterize topological insulating phases. Our findings open an avenue for the exploration of topological insulators of SU($N \geq 3$) fermions with and without interactions, and also suggest that such phases may be found in lattice quantum chromodynamics models.

One of us (C.A.R.S.d.M.) would like to thank the support of the Galileo Galilei Institute for Theoretical Physics via a Simons Fellowship, and of the International Institute of Physics via the Visitor's Program.

-
- [1] D. J. Thouless, M. Kohmoto, M. P. Nightingale, and M. den Nijs, Quantized Hall Conductance in a Two-Dimensional Periodic Potential, *Phys. Rev. Lett.* **49**, 405-408 (1982).
- [2] M. Kohmoto, Topological Invariant and the Quantization of the Hall Conductance, *Ann. Phys.* **160**, 343 (1985).
- [3] Y. Hatsugai, Chern Number and Edge States in the Integer Quantum Hall Effect, *Phys. Rev. Lett.* **71**, 3697 (1993).
- [4] Y. Hatsugai, Topological aspects of the quantum Hall effect, *J. Phys.: Condens. Matter* **9**, 2507 (1997).
- [5] C. L. Kane and E. J. Mele, Z_2 Topological Order and the Quantum Spin Hall Effect *Phys. Rev. Lett.* **95**, 146802 (2005).
- [6] Y. Yang, Z. Xu, L. Sheng, B. Wang, D. Y. Xing, and D. N. Sheng, Time-Reversal-Symmetry-Broken Quantum Spin Hall Effect, *Phys. Rev. Lett.* **107**, 066602 (2011).
- [7] W. Beugeling, N. Goldman, and C. Morais Smith, Topological Phases in a Two-dimensional Lattice: Magnetic Field versus Spin-orbit Coupling, *Phys. Rev. B* **86**, 075118 (2012).
- [8] S. Taie, R. Yamazaki, S. Sugawa, Y. Takahashi, An SU(6) Mott insulator of an Atomic Fermi Gas Realized by Large-spin Pomeranchuk Cooling, *Nature Physics* **8**, 825 (2012).
- [9] H. Ozawa, S. Taie, Y. Takasu, and Y. Takahashi, Antiferromagnetic Spin Correlation of SU(N) Fermi Gas in an Optical Superlattice, *Phys. Rev. Lett.* **121**, 225303 (2018).
- [10] G. Pagano, M. Mancini, G. Cappellini, P. Lombardi, F. Schäfer, H. Hu, X. J. Liu, J. Catani, C. Sias, M. Inguscio, and L. Fallani, A One-dimensional Liquid of Fermions with Tunable Spin, *Nature Physics* **10**, 198 (2014).
- [11] L. F. Livi, G. Cappellini, M. Diem, L. Franchi, C. Clivati, M. Frittelli, F. Levi, D. Calonico, J. Catani, M. Inguscio, and L. Fallani, Synthetic Dimensions and Spin-Orbit Coupling with an Optical Clock Transition, *Phys. Rev. Lett.* **117**, 220401 (2016).
- [12] F. Scazza, C. Hofrichter, M. Höfer, P. C. De Groot, I. Bloch, and S. Fölling, Observation of Two-orbital Spin-exchange Interactions with Ultracold SU(N)-symmetric Fermions, *Nature Physics* **10**, 779 (2014).
- [13] C. Hofrichter, L. Riegger, F. Scazza, M. Höfer, D. R. Fernandes, I. Bloch, and S. Fölling, Direct Probing of the Mott Crossover in the SU(N) Fermi-Hubbard Model, *Phys. Rev. X* **6**, 021030 (2016).
- [14] M. Aidelsburger, M. Atala, M. Lohse, J. T. Barreiro, B. Paredes, and I. Bloch, Realization of the Hofstadter Hamiltonian with Ultracold Atoms in Optical Lattices, *Phys. Rev. Lett.* **111**, 185301 (2013).
- [15] Hirokazu Miyake, Georgios A. Siviloglou, Colin J. Kennedy, William Cody Burton, and Wolfgang Ketterle, Realizing the Harper Hamiltonian with Laser-Assisted Tunneling in Optical Lattices, *Phys. Rev. Lett.* **111**, 185302 (2013).
- [16] Y. J. Lin, K. Jimenez-Garcia, and I. B. Spielman, Spin-orbit coupled Bose-Einstein condensates, *Nature (London)* **471**, 83 (2011).
- [17] N. Goldman, I. Satija, P. Nikolic, A. Bermudez, M. A. Martin-Delgado, M. Lewenstein, and I. B. Spielman, Realistic Time-Reversal Invariant Topological Insulators with Neutral Atoms, *Phys. Rev. Lett.* **105**, 255302 (2010).
- [18] P. G. Harper, Single Band Motion of Conduction Electrons in a Uniform Magnetic Field, *Proc. Phys. Soc. London Sect. A* **68**, 874 (1955).
- [19] D. M. Kurkcuoglu, Theoretical Aspects of Ultra-Cold Fermions in the Presence of Artificial Spin-Orbit Coupling, Ph.D. Thesis, Georgia Institute of Technology, (2015).
- [20] D. M. Kurkcuoglu, and C. A. R. Sá de Melo, Creating Spin-One Fermions in the Presence of Artificial Spin-Orbit Fields: Emergent Spinor Physics and Spectroscopic Properties, *J. Low Temp. Phys.* **191**, 174 (2018). See also arXiv:1609.06607v1 (2016).
- [21] D. M. Kurkcuoglu, and C. A. R. Sá de Melo, Color Superfluidity of Neutral Ultracold Fermions in the Presence of Color-flip and Color-orbit Fields, *Phys. Rev. A* **97**, 023632 (2018).
- [22] We note that the Hamiltonian in Eq. (7) in general does not commute with the Gell-Mann matrices λ_j , which are the eight generators of SU(3). To see this explicitly, it is

- sufficient to recall that the angular momentum matrices \mathbf{J}_ℓ can be written in terms of λ_j as $\mathbf{J}_x = (\lambda_1 + \lambda_6)/2$; $\mathbf{J}_y = (\lambda_2 + \lambda_7)/2$; and $\mathbf{J}_z = (\lambda_3 + \sqrt{3}\lambda_8)/2$ and to show that the commutator $[\hat{\mathbf{H}}, \lambda_j] \neq 0$.
- [23] Q. Niu, D. J. Thouless, and Y. S. Wu, Quantized Hall Conductance as a Topological Invariant, *Phys. Rev. B* **31**, 3372 (1985).
- [24] D. N. Sheng, L. Balents, and Z. Wang, Phase Diagram for Quantum Hall Bilayers at $\nu = 1$, *Phys. Rev. Lett.* **91**, 116802 (2003).
- [25] D. N. Sheng, Z.Y. Weng, L. Sheng, and F. D. M. Haldane, Quantum Spin-Hall Effect and Topologically Invariant Chern Numbers, *Phys. Rev. Lett.* **97**, 036808 (2006).
- [26] E. Zhao, N. Bray-Ali, C. J. Williams, I. B. Spielman, and I. I. Satija, Chern Numbers Hiding in Time-of-flight Images, *Phys. Rev. A* **84**, 063629 (2011).
- [27] H. M. Price, and N. R. Cooper, Mapping the Berry Curvature from Semiclassical Dynamics in Optical Lattices, *Phys. Rev. A* **85**, 033620 (2012).
- [28] A. Dauphin, and N. Goldman, Extracting the Chern Number from the Dynamics of a Fermi Gas: Implementing a Quantum Hall Bar for Cold Atoms, *Phys. Rev. Lett.* **111**, 135302 (2013).
- [29] G. Jotzu, M. Messer, R. Desbuquois, M. Lebrat, T. Uehlinger, D. Greif and T. Esslinger, Experimental Realization of the Topological Haldane Model with Ultracold Fermions, *Nature* **515**, 237 (2014).
- [30] M. Aidelsburger, M. Lohse, C. Schweizer, M. Atala, J. T. Barreiro, S. Nascimbene, N. R. Cooper, I. Bloch and N. Goldman, Measuring the Chern number of Hofstadter Bands with Ultracold Bosonic Atoms, *Nature Phys.* **11**, 162 (2015).